

## Passivity-Based Integral Control for Stability Evaluation: An Application to Microgrid

G. Kusuma

Department of Electrical and Electronics Engineering,  
Andhra University College of Engineering (A)  
Visakhapatnam, A.P, India-530003.

T. R. Jyothsna

Department of Electrical and Electronics Engineering,  
Andhra University College of Engineering (A)  
Visakhapatnam, A.P, India-530003.

### Abstract

*In this paper, a nonlinear passivity based integral controller that ensures the stability for the photovoltaic (PV) inverter based microgrid is developed. Based on the passive integral control theory a new positive semi definite storage function is obtained to form an energy-like Lyapunov function. This storage function results in a new integral control law and the obtained Lyapunov argument is used for designing globally stabilizing controller that is capable of handling system perturbation as well as transients. To test the correctness of the proposed controller, a microgrid consisting of three photovoltaic distributed generation sources (DGS) has been considered. The microgrid model that is considered in the paper gathers the information on the control loops of the photovoltaic DG but not the switching action. Numerical simulations are then furnished to assess the application of this control to the inverter based microgrid with three 10 KVA PV inverters and the accuracy of the controller is verified for steady state and large signal variations.*

**Index Terms**—Passivity based integral controller, Lyapunov argument, large signal variations, microgrid, PV inverter, storage function.

### INTRODUCTION

MICROGRID is a local grid with small-scale distributed power generation systems combined with power electronic systems, energy storage systems (ESS), and local loads with capability to operate in either grid-connected or standalone mode. These small standalone power systems can integrate renewable energy, other

forms of DGS and thereby interface to the network through power conditioning equipment. These interface devices make the sources more flexible in their operation and control and hence increase the reliability and efficiency of the microgrid.

Several controllers have been proposed in the literature for the design of power conditioning equipment so as to enhance the voltage quality of microgrid. The discrete dynamical modeling of the PV system in accordance to the system energy-balance principle has been analyzed in [4]. An energy-sampled data model of a grid-connected PV system with cascade H-bridge multilevel converter has been investigated in [1]. The control scheme for grid-connected PV systems with DC-link based inverters has been assessed in [2]. An accurate model of the dynamic behavior of PV generating units by representing the system's response to variations in irradiance and ac grid voltage has been evaluated in [5]. A linear large-signal energy-sampled data model is obtained that allows for the extraction of maximum energy from the PV array has been proposed [3]. However, in all the above work, different system perturbations, various load conditions and transients have not been considered.

In [6], a seamless control structure for a PV-Diesel microgrid has been suggested to operate it both in the grid connected and in the isolated mode. A hybrid ac/dc micro grid which consists of ac and dc networks

**Cite this article as:** G. Kusuma & T. R. Jyothsna, "Passivity-Based Integral Control for Stability Evaluation: An Application to Microgrid", International Journal & Magazine of Engineering, Technology, Management and Research, Volume 4 Issue 1, 2017, Page 581-591.

integrated through bidirectional converters has been investigated in [7]. However, global stability may not be ensured as the controllers considered are of PI type in all the above work.

The Lyapunov-based control approach has been illustrated in [8]. A new control strategy for single-phase shunt Active Power Filters (APFs) based on Lyapunov's stability theory has been proposed in [9] so as to obtain the global stability of the system for steady and transient variations. In [10] a control method based on Lyapunov's direct method to stabilize the system globally to handle large signal disturbances has been described. A passivity-based controller for the closed-loop regulation of a class of DC-DC power converters by considering a resistive load has been developed in [11]. A robust adaptive voltage controller for a three-phase inverter has been proposed in [12] by taking into account the perturbations of system parameters.

In [13] the modeling and analysis of standalone inverter-based microgrids has been developed. To enhance the stability of dc microgrids with Constant Power Loads (CPL) virtual-impedance-based stabilizers are proposed in [14]. An iterative distributed algorithm previously is developed in [15] to operate each DER independently within an environment that allows the microgrid to dynamically adapt to changes in the real-time operating environment. In this paper [16], P-Q and P-V controls for solar arrays are discussed. A hybrid ac/dc microgrid in [17] is proposed by considering perturbation and dynamic characteristics of wind speed, solar irradiance, ambient temperature, and load conditions. However, in all this work attaining global stability is a problem.

A suitable networked control framework has been developed in [18] for controlling the electromechanical oscillations in power systems. In this paper [19] the power flow control and management issues amongst multiple sources dispersed throughout both ac and dc microgrids through a decentralized power sharing method has been considered. A standalone microgrid containing both controllable and uncontrollable sources, like solar, wind, diesel generator, fuel cell, aqua-

electrolyser, hydrogen storage and battery is considered in [20]. This paper [21] has shown that passivity-based integral control is one of solutions for regulating DC-to-DC converters for large-signal variations and also ensures global stability. The design of a proportional passive controller as well as the major challenges in microgrid control, and a review of control strategies and trends which guarantees the global stability of the system is presented in [22]-[27].

After a careful and extensive literature survey, this paper proposes a new passive integral controller for the PV inverter in a standalone microgrid and has been tested under various perturbations, different load conditions and severe transients. First, the state-space model of the three-phase inverter is which considers the perturbations of system parameters are derived. Inverter inner control loop is designed based on the passivity-based integral law and tracking of outer loop is performed to eliminate high frequency disturbances. The small-signal state-space model of an inverter along with the controller is first modeled and then the control law is designed. The controller designed is incorporated in the microgrid test system [13] and has then been examined for various large signal disturbances and it is proved through the MATLAB simulation that with the proposed closed-loop control system the test system is globally stable.

## **PHOTOVOLTAIC DGS MODEL AND CONTROL STRATEGY**

Fig. 1 shows the schematic diagram of a standalone photovoltaic DGS which consists of the photovoltaic generator, a three-phase dc-ac inverter, an LC output filter, a coupling inductor and a local load. The objective of these power electronics components is to derive maximum extraction of energy from the photovoltaic generator.

This paper concentrates on design and development of a new passivity-based integral current controller for various types of PV operating conditions, perturbations in states, and different loading condition. The LC output filter in this circuit plays a significant role in eliminating harmonic components of the inverter output voltage

caused by high-frequency switching actions. In the above system the modeling of PV, the PV inverter, LC output filter, a coupling inductor is shown in the sections below:

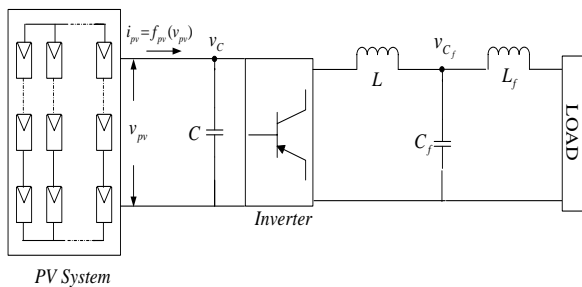


Fig.1. Standalone Photovoltaic DGS.

### PV Modeling

The electrical behavior of a PV cell [22] can be represented as an ideal p-n junction in parallel with a constant current which is depicted in Fig. 2 can be represented as:

$$i_{cell} = I_{gc} - I_{sat} \left[ \exp\left(\frac{V_{cell}}{\eta V_T}\right) - 1 \right] \quad (1)$$

The current source  $I_{gc}$  represents the light-induced current and the current flowing through the diode,  $i_d$ , can be derived from the equations of an ideal p-n junction:

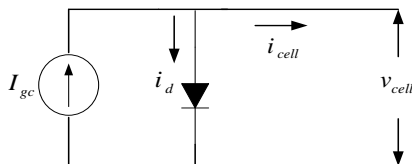


Fig.2. Ideal Model of a PV cell.

$$i_d = I_{sat} \left[ \exp\left(\frac{V_{cell}}{\eta V_T}\right) - 1 \right] \quad (2)$$

where  $\eta$  is the emission coefficient which depends on semiconductor material of the cell,  $I_{sat}$  is the reverse saturation current of the p-n junction and  $V_T$  is the thermal voltage defined as

$$V_T = \frac{k_B T_{cell}}{q_e} \quad (3)$$

here,  $k_B$  and  $q_e$  are the Boltzmann constant and the electron's charge and  $T_{cell}$  represents the cell's temperature respectively.

The output current from the photovoltaic generator,  $i_{pv}$  which is dependent on  $v_{pv}$  can be represented as:

$$f_{pv}(v_{pv}) = i_{pv} = \lambda - \psi \exp(\alpha v_{pv}) \quad (4)$$

where

$$\lambda = (I_{gc} + I_s)n_p; \psi = I_s n_p; \alpha = \frac{n_s}{\eta V_T}$$

where  $\psi, \alpha$  represents non-negative parameters of the photovoltaic generator and  $\lambda$  represents the part of photovoltaic generator current that only depends on external variables (e.g. the solar irradiance).  $n_s$  and  $n_p$  are the number of PV panels connected in series and parallel, respectively. The details of PV system parameters are shown in Table I.

TABLE I  
LCL filter parameters:

Parameters	Value
$C_f$	50 $\mu$ F
$L_f$	1.35mH
$C$	2.2 mF
$L$	1.0 mH

TABLE II

PV system parameters at irradiance 1000 $Wm^{-2}$	
Parameters	Value
$\psi$	$1.35e^{-7}A$
$\lambda$	14.1A
$\alpha$	$0.026/^{\circ}C$

### PV Inverter Modeling

The schematic diagram of the full-bridge inverter considered in the present work is shown in Fig. 3(a). This configuration consists of switches controlled by a switching signal  $\delta \in \{0, 1\}$  (i.e., OFF or ON respectively) as well as an assumption that there is a control signal  $u \in \{-1, 1\}$  such that  $\delta = (u+1)/2$ . From Fig. 1, it can be found that,  $x_1 = v_{pv}$  and  $x_2 = i_L$  are the instantaneous input capacitor voltage and the output inductor current, respectively.

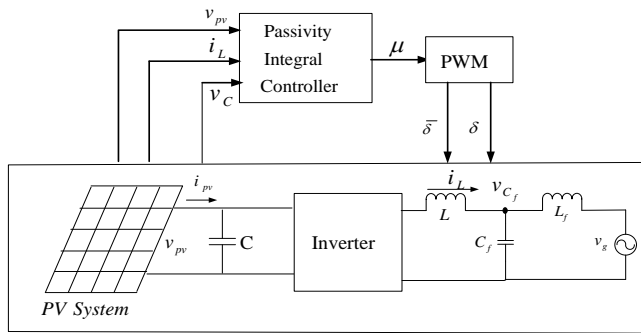
Then the system dynamic equations for the PV inverter represented in Fig. 1 can be written as follows:

$$\begin{aligned} C \frac{dx_1}{dt} &= -ux_2 + f_{pv}(x_1) \\ L \frac{dx_2}{dt} &= ux_1 - V_{C_f} \end{aligned} \quad (5)$$

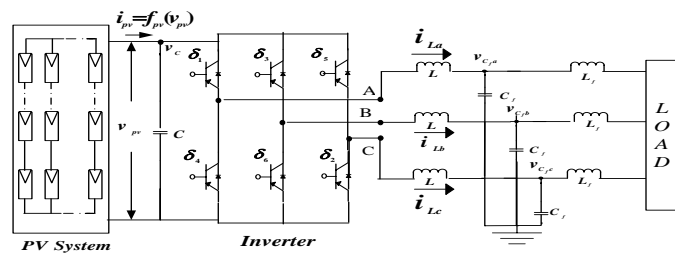
where  $f_{pv}(x_1)$  is given by (4)

The switching signal  $\delta$  can also be generated via a pulse-width modulator (PWM) scheme with an input signal  $\mu$

$\in [-1, 1]$  obtained as output by the controller. In this case, if the switching frequency is sufficiently high, the dynamical behaviour of the PV inverter system can be approximated by the following set of differential equations in Fig. 3:



(a)



(b)

Fig.3.a ) Typical Control Scheme of a Photovoltaic DGS.b )Three Phase PV Inverter System.

$$C \frac{dz_1}{dt} = -uz_2 + f_{pv}(z_1)$$

$$L \frac{dz_2}{dt} = uz_1 - V_{C_f} \quad (6)$$

where  $z_1$  and  $z_2$  are the averaged values of  $x_1$  and  $x_2$ , which represents the voltage across the capacitor ( $v_{pv}$ ) and current through the inductor ( $i_L$ ) respectively.

Filter and coupling inductor Modeling

The LC output filter plays a role in eliminating harmonic components of the inverter output voltage caused by high-frequency switching actions. The filter shown in Fig. 1 yields the following state equations by using Kirchhoff's voltage and current laws:

$$\frac{dV_{C_f}}{dt} = \frac{1}{C_f} (i_L - i_{L_f})$$

$$\frac{di_{L_f}}{dt} = \frac{1}{L_f} (V_{C_f} - v_g) \quad (7)$$

The utility grid voltage  $V_g$  is assumed to be sinusoidal with a constant amplitude  $A$  and a constant frequency  $\omega$ , i.e.,  $V_g = A \sin(\omega t)$ . The microgrid modelling approach in this work is to form a sub-model of all the individual DG inverters connected remotely and combine them with the network and individual load models as in [13]. The details of system parameters considered in (6), (7) as well as the microgrid test system in Fig. 4 are shown in Tables I and II.

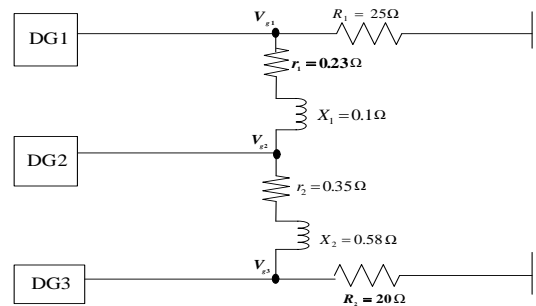


Fig.4. Microgrid Test System.

PASSIVITY-BASED INTEGRAL CONTROLLER FOR THE PV INVERTER

In this section the passivity-based control of a system which consists of a passive output and also an integral function (10) is developed for the PV inverter. The integral function is the variable to be regulated since it consists of the capacitor voltage error. To perform this, combined storage functions are developed for system (8-9) so that a new integral control can be obtained that ensures asymptotic stability for large signal perturbations. The storage function defined in (12) would be combined with a new one in (13), which includes an integral term. The dynamics of the incremental values for the PV inverter described in (6) are given by:

$$z_1 = z_{1s} + z_{1p}; z_2 = z_{2s} + z_{2p}; \mu = \mu_s + \mu_p \quad (8)$$

where  $z_{1p}$ ,  $z_{2p}$  and  $\mu_p$  are perturbations,  $z_{1s}$ ,  $z_{2s}$  and  $\mu_s$  are steady state values in  $z_1$ ,  $z_2$ ,  $\mu$  respectively.

$$\frac{dz_{1p}}{dt} = \frac{1}{C} [-\mu_p (z_{2s} + z_{2p}) - \mu_s z_{2p} f_{pvp}]$$

$$\frac{dz_{2p}}{dt} = \frac{1}{L} [\mu_p(z_{1s} + z_{1p}) + \mu_s z_{1p}] \quad (9)$$

$$\frac{dz_{3p}}{dt} = z_{1p} \quad (10)$$

$z_{3p}$  is the integral of the voltage incremental error.

Thus, consider the following storage function.

$$V(x) = V_1(x) + V_2(x) \quad (11)$$

Choosing,

$$V_1(x) = \frac{1}{2} C z_{1p}^2 + \frac{1}{2} L z_{2p}^2 \quad (12)$$

$$V_2(x) = \frac{1}{2} \beta^2 z_{1p}^2 \quad (13)$$

The above storage function is positive definite and unbounded for the inverter dynamics considered in (11), and its time-derivative is

$$\frac{dV(x)}{dt} = \frac{dV_1(x)}{dt} + \frac{dV_2(x)}{dt} \quad (14)$$

Upon substituting equations (8)-(10) into (12)-(13) respectively, we obtain

$$\frac{dV_1(x)}{dt} - z_{1p} f_{pvp} = -\mu_p(z_{1p} z_{2s} - z_{1s} z_{2p}) \quad (15)$$

$$\frac{dV_2(x)}{dt} = \beta^2 z_{1p} \frac{dz_{1p}}{dt} \quad (16)$$

Hence from (15) and (16),

$$\begin{aligned} \frac{dV(x)}{dt} = & -\mu_p(z_{1p} z_{2s} - z_{1s} z_{2p}) + z_{1p} f_{pvp} + \\ & \frac{\beta^2}{C} [-\mu_p(z_{1p} z_{2s} - z_{1p} z_{2p}) - \mu_s z_{1p} z_{2p} \\ & + z_{1p} f_{pvp}] \quad (17) \end{aligned}$$

With the following output

$$\begin{aligned} \frac{dV(x)}{dt} = & -\mu_p(z_{1p} z_{2s} - z_{1s} z_{2p}) + z_{1p} f_{pvp} + \\ & K [-\mu_p(z_{1p} z_{2s} - z_{1p} z_{2p}) - \mu_s z_{1p} z_{2p} + z_{1p} f_{pvp}] \quad (18) \end{aligned}$$

where  $K = \beta^2/C$ ; using  $\mu_p = -\mu_s$ ; we get

$$\begin{aligned} \frac{dV}{dt} = & z_{1p} f_{pvp} (1 + K) + \mu_p (z_{1s} z_{2p} \\ & - z_{1p} z_{2s} (1 + K)) \quad (19) \end{aligned}$$

Then (19), becomes

$$\frac{dV(x)}{dt} \leq y \mu_p \quad (20)$$

wherechoosing the following passive output as

$$y = z_{1s} z_{2p} - z_{1p} z_{2s} (1 + K)$$

and the passive input-output behavior is proved. A memory-less function  $\Phi(\cdot)$  is introduced, that represents a feedback gain and takes saturation into account,

$$\mu_p = -\Phi y \quad (21)$$

And we shall define  $K = \beta^2/C$ , where  $\beta$  and  $\mu_p$  are constant values. Therefore, the control law is proposed as:

$$\mu_p(S) = -\Phi(z_{1s} z_{2p} - (1 + K) z_{1p} z_{2s}) \quad (22)$$

which guarantees the global asymptotic stability of the controller. Once the nonlinear control law has been established,  $\Phi$  and  $K$  will be selected to ensure that the controller behaves satisfactorily in small-signal operation. By linearizing the control law (22), we obtain:

$$\begin{aligned} \mu_{plin}(S) = & -\Phi_{max} (z_{1s} z_{2p}(S) \\ & - (1 + K) z_{1p}(S) z_{2s}) \quad (23) \end{aligned}$$

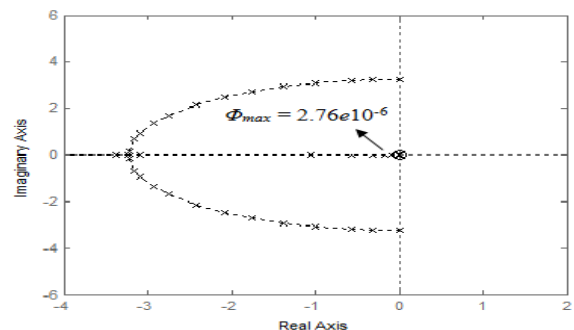


Fig. 5. Root loci for gain loop of equation (23).

The corresponding loop gain is given by

$$\begin{aligned} T(S) \\ = & -\Phi_{max} \left[ \frac{(z_{1s}^2 CS + (1 + K) z_{2s}^2 LS + K \mu_s z_{1s} z_{2s})}{(LCS^2 + \mu_s^2)} \right] \quad (24) \end{aligned}$$

Detailed controller equations are shown in Appendix I. Asymptotically, the decay of the Lyapunov function  $V(x)$  is controlled by the eigenvalues of the small signal model obtained by linearizing the closed-loop system about  $x = 0$ . This is useful in choosing gain  $K$ , thereby obtaining flexibility in placing the eigenvalues of the linearized closed-loop system in the left of the plane as shown in Fig. 5. From the root locus plot in Fig. 5,

represented in (24), again value of  $K=500$  and the  $\phi_{max}$  within the interval  $[1e^{-8}-3e^{-6}]$  are obtained.

## MICROGRID SIMULATION

The Lyapunov-based Passivity-Based Integral Control method described in [8] has been extended to applications in distributed power supply environments as this type of control proves to be very useful as it has become necessary to stabilize arbitrary interconnections of inverters and loads.

In this work, a prototype 30 KVA micorgid system is considered to implement the proposed adaptive integral voltage control algorithm. The 220 V (per phase RMS), 50 Hz test system consist of three inverters of equal rating (10 kVA) with two load banks, one at each bus 1 and bus 3. The test system has the following system parameters as given in Table I. The inverters are controlled to share the real and reactive powers over the lines 1 and 2. In the test system resistive loads were used to evaluate the model. A resistive load each of 7.3 kW (20  $\Omega$  per phase each) at buses 1 and 3 is an initial operating condition.

The simulation results of the proposed voltage controller are obtained using MATLAB under various different conditions. The simulation results are aimed at exhibiting the behavior of the controller for perturbations in system states, as well as loadresistance variations which is considered unknown. The operations of the microgridunder various source, load and short circuit conditions are simulated to verify the behavior of the proposed control. All the waveforms illustrated in the case studies below represent the MATLAB simulation of the control law (23) with  $\Phi_{max}=2.76X10^{-6}$ , which was chosen for settling time minimization.

### Case Study I: Impact of PV Irradiance

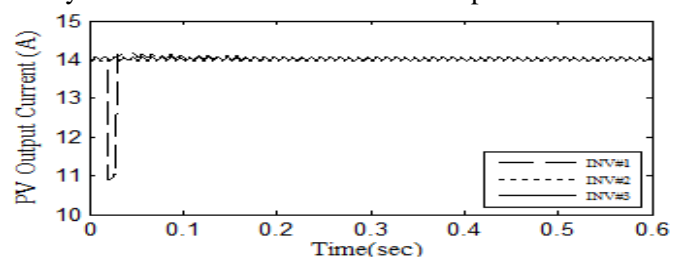
This case assesses the situation when the system is subjected to the changing solar irradiance. The adopted PV array model described in (4) is represented as,

$$f_{pv}(v_{pv}) = i_{pv} = \lambda - \psi \exp(\alpha v_{pv})$$

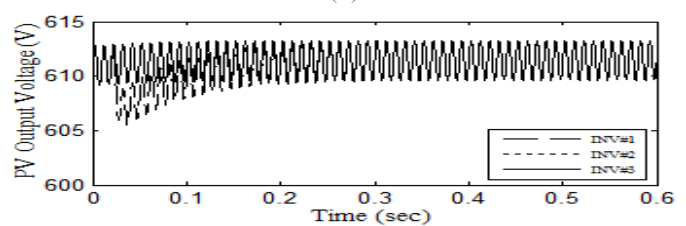
where  $\lambda$  depends on the solar incident irradiance,  $\psi$  depends on the PV cells' semiconductor material and  $\alpha$  depends on the PV panels' temperature and the PV cells' semiconductor material. The parameter that varies the most is  $\lambda$ , as the solar irradiance changes significantly during any day. On the other hand, parameters  $\psi$  and  $\alpha$  changes less frequently than  $\lambda$  and can also be measured easier and cheaper than measuring  $\lambda$ .

Figs. 6(a) through 6(d) shows the system response when the input PV irradiance has step changes in inverter #1, first it decreases from 14.1 to 13.1 and then returns to the original value. During this short transient there is a small undershoot across the PV output current, voltage, and the output power, as the output from a PV cell depends on the level of radiation. After the disturbance has been removed, all the signals return to the desired constant system output with almost zero steady-state error, showing the steady state behaviour of the system.

Figs. 7(a) through 7(d) shows when there are perturbations in irradiance for the inverters #1 and #3 simultaneously while there is no irradiance change across inverter #2. These perturbations in irradiance again affect the PV voltage, current and DC output power of PV across these inverters. It can be observed in all the waveforms that the system behaves robustly by returning to the desired output voltage with almost zero steady-state error after a short transient period.



(a)



(b)

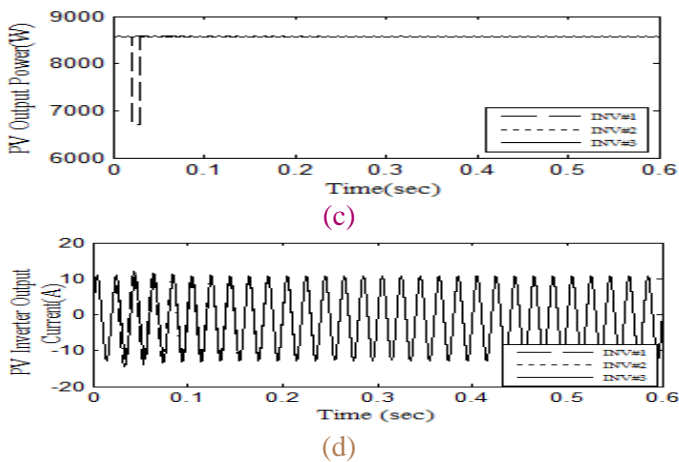


Fig.6. Perturbation in PV irradiance for inverter 1. a) DC Output current of PV. b) DC Output voltage of PV. c) DC output power of PV. d) PV Inverter current.

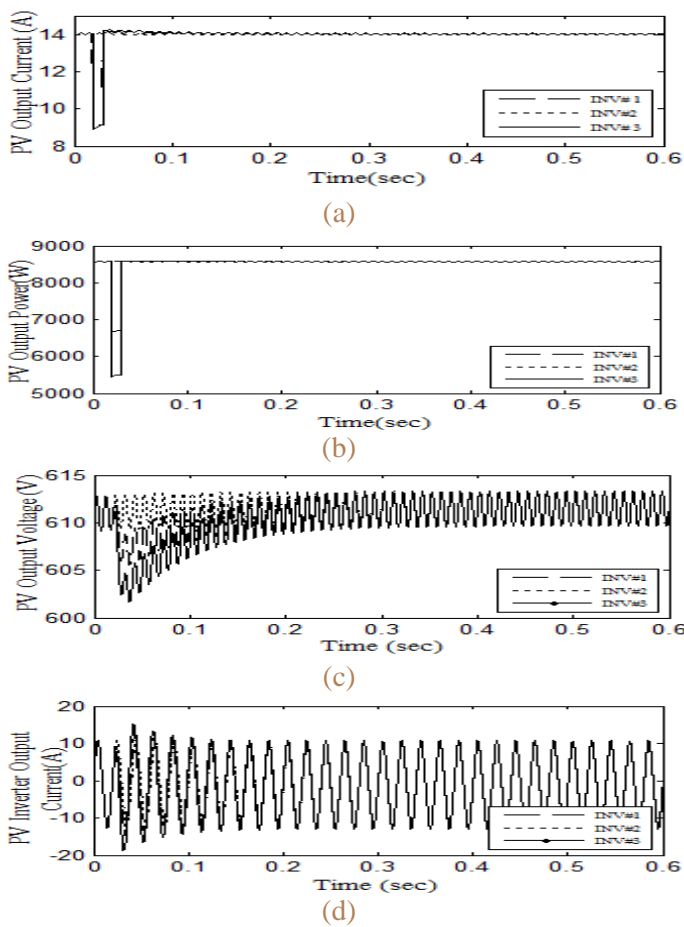


Fig.7. Perturbation in PV irradiance for inverters 1 and 3. a) DC Output current of PV. b) DC Output voltage of PV. c) DC output power of PV. d) PV Inverter current.

### Case Study II: Assessment of Parameter Perturbation

In order to evaluate the performance of the passive integral controller with parameter Perturbation, the capacitance voltage across the PV source ( $Z_1$ ) and inductance current ( $Z_2$ ) through the output filter is changed. In particular, the system state parameters are perturbed with 20-25% variations from their nominal values. During the transients initiated in all the inverters at a time instant of 0.05 sec, there is deviation in the capacitance voltage across PV i.e.,  $Z_1$  as observed in the Figs. 8(a) and 8(b). It is noted that the DC voltage component across the capacitor Fig.8(a) approaches asymptotically for all the inverters. Also, the inductor current in Fig. 8(b) recovers quickly after a short duration. Figs. 9(a) and 9(b) show the perturbations in inductor current  $Z_2$ , initiated in all the inverters at a time instant of 0.05 sec across the PV inverter. It can be observed there is an overshoot in current of about 60-80 A as in Fig. 9(b) when there is perturbation and the robustness of controller is capable of making the system to return almost to the original operating point quickly as observed in the Figures.

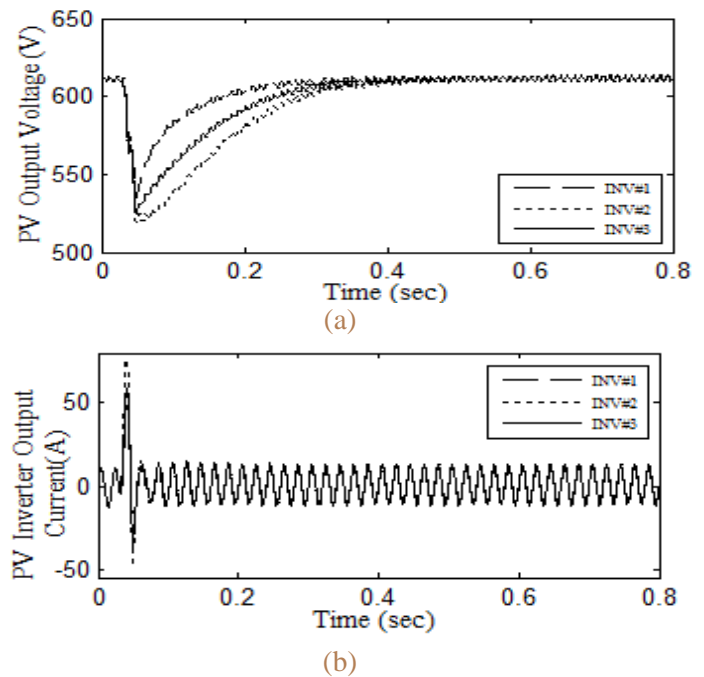


Fig.8. System Waveforms for Perturbations in PV output voltage ( $Z_1$ ). a) PV output voltage ( $Z_1$ ). b) PV inverter current ( $Z_2$ ).

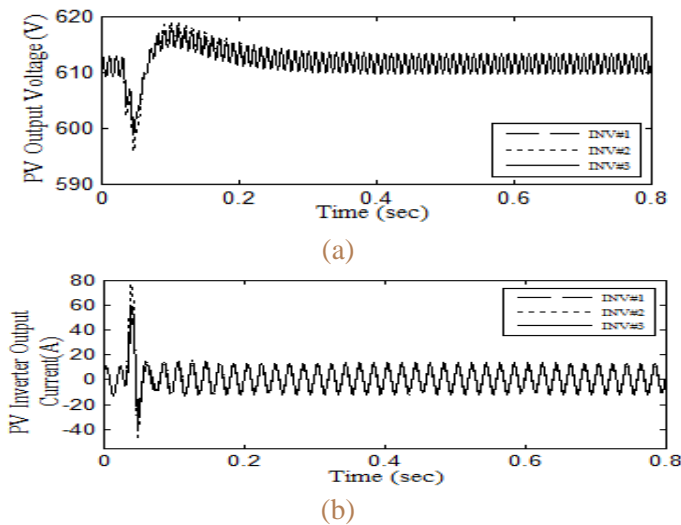


Fig. 9. System Waveforms for Perturbations in PV inverter current ( $Z_2$ ) across all 3 inverters. a) PV output voltage ( $Z_1$ ). b) PV inverter current ( $Z_2$ ).

### Case Study III: Short circuit fault at MicroGrid Terminal

The proposed passive controller is tested for a severe disturbance, a three-phase to ground fault at the terminals of the grid. The disturbance is initiated at  $t = 0.02$  second and is cleared within 0.03 seconds as shown in Figs. 10(a) through 10(c). During the time of the fault, there is deviation in the system parameters from the steady operating point depicting the intensity of three-phase to ground fault; It is evident from Fig. 10(a) and 10(c), the output voltage as well as the active output power across the inverter terminal is zero during which time there is an overshoot in the inverter output current as in Fig. 10(b). As soon as the fault is cleared, the system has regained to its steady point quickly.

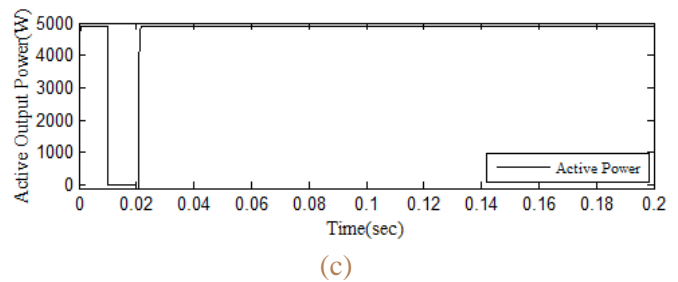
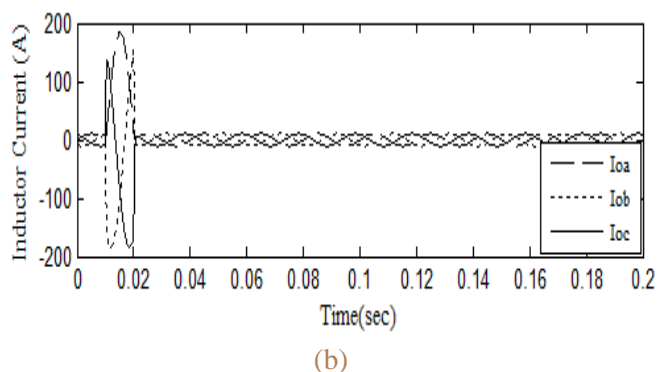


Fig. 10. System Waveforms for a short circuit at Microgrid Terminal for inverter 1. a) Capacitor (filter) output voltage ( $Z_1$ ). b) Inductor (filter) current. c) PV inverter real power.

### Case Study IV: Change in Load Variations

The disturbance is considered as a step decrease in load resistance from 20 to 19 ohms at bus 3 as shown in Figs. 11(a) and 11(b). In Fig. 11(a) it can be seen that DG3, which is closer to the varying load, has taken a larger share of the load whereas DG1 and DG2 have taken a slightly lighter load, depending on the effective impedance seen from the load point. Hence, during large load variations, closely located DGs may be overloaded. Also in Fig. 11(b) the load current takes larger part of current during transient.

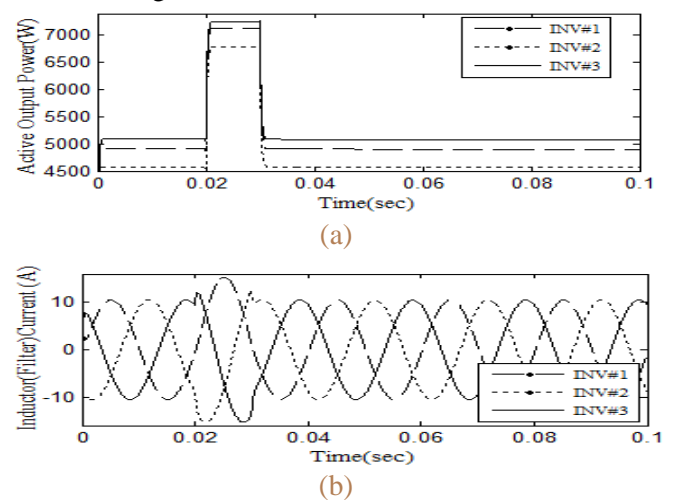


Fig. 11. System Waveforms for a step decrease in load from  $20 \Omega$  to  $19 \Omega$ . a) PV inverter real power ( $Z_{1p}$ ). b) Inverter currents.

Figs. 12(a) and 12(b) depict the results of the microgrid for a step-increase of load resistance from  $20 \Omega$  to  $21 \Omega$  at bus 3. The decrease in load currents as well as the load



active power of all the three inverters is clearly visible. The waveforms are expressed in abc reference frames.

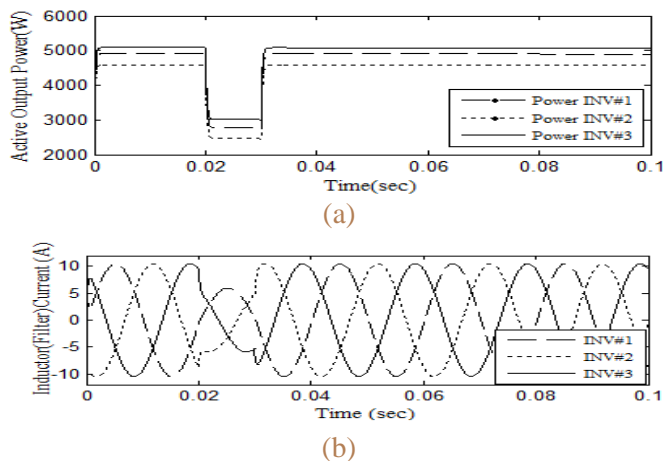


Fig. 12. System Waveforms for a step-increase in load from  $20 \Omega$  to  $21 \Omega$ . a) PV inverter real power ( $Z_{ip}$ ). b) Inverter (Filter) currents.

## CONCLUSION

This paper has designed and developed a robust passive integral control strategy applied for the first time to a standalone Photovoltaic microgrid. The proposed controller is easier to implement, and is also robust to perturbations in PV operating conditions, system perturbations, as well as sudden load variations. This is evident from the mathematical model of the proposed integral controller applied to the system microgrid and the obtained simulation results. The investigation of the simulation results demonstrated that the proposed integral controller is versatile in all aspects of fast dynamic response, negligible steady-state error and different load conditions in the presence of the perturbations of microgrid test system.

## REFERENCES

[1] J.J.Negroni, Carlos Meza, Domingo Biel, and F.Guinjoan, "Energy-Sampled Data Modeling of a Cascade H-Bridge Multilevel Converter for Grid-Connected PV Systems." In IEEE International Symposium on Power Electronics, Puebla, Mexico, pp.1-6, October 16-18, 2006.

[2] Carlos Meza, J.J.Negroni, D.Biel and F.Guinjoan, "Considerations on the Control Design of DC-link based Inverters in Grid –Connected Photovoltaic Systems." In IEEE International Symposium on Circuit and Systems, ISCAS-2006, island of Kos, pp.5070-5073, May 21-24, 2006.

[3] Carlos Meza, J.J.Negroni, D.Biel and F.Guinjoan, "Inverter Configuration Comparative for Residential PV Grid-Connected Systems." In IEEE International Symposium on Industrial Electronics, IECON-2006, pp.4361-4366, November 6-10, 2006.

[4] Carlos Meza, J.J.Negroni, D.Biel and F.Guinjoan, "Energy-Balance Modelling and Discrete Control for Single –Phase Grid –Connected PV Central Inverters." In IEEE International Transactions on Industrial Electronics, Volume:55, Issue: 7, pp.2734-2743, July 2008.

[5] Yun Tiam Tan, Daniel S.Kirschen and Nicholas Jenkins, "A Model of PV Generation Suitable for Stability Analysis." In IEEE International Transactions on Energy Conversion, Volume:19, Issue: 4, pp.748-755, December 2004.

[6] S.Mishra, D.Ramasubramanian and P.C.Sekhar, "A Seamless Control Methodology for a Grid Connected and Isolated PV-Diesel Microgrid." In IEEE International Transactions on Power Systems, Volume:28, Issue: 4, pp.4393-4404, November 2013.

[7] Xiong Liu, Peng Wang and Poh Chiang Loh, "A Hybrid AC/DC Microgrid and Its Coordination Control." In IEEE International Transactions on Smart Grid, Volume:2, Issue: 2, pp.278-286, June 2011.

[8] Seth R Sanders and George C.Vergheze, "Lyapunov-Based Control for Switched Power Converters." In IEEE International Transactions on Power Electronics, Volume:7, Issue: 1, pp.17-24, January 1992.

[9] HasanKomurcugil and Osman Kukrer, "A New Control Strategy for Single –Phase Shunt Active Power Filters Using a Lyapunov Function" In IEEE International Transactions on Industrial Power Electronics, Volume:53, Issue: 1, pp.17-24, February 2006.

- [10] HasanKomurcugil and Osman Kukrer, “Control Strategy for Single –Phase PWM ac/dc Voltage-Source Converters based on Lyapunov’s direct method.” In Taylor & Francis on International Journal of Electronics,87:12,, pp.1485-1498, November 2010.
- [11] G.Escobar, D.Chevreau, R.Ortega and E.Mendes, “An Adaptive Passivity-Based Controller for a Unity Power Factor Rectifier.” In IEEE International Transactions on Control Systems Technology,Volume:9, Issue: 4, pp.637-644, July 2001.
- [12] Jin-Woo Jung, NgaThi-Thuy Vu, Dong Quang Dang, Ton DucDo,Young-Sik Choi and Han Ho Choi, “A Three –Phase Inverter for a Standalone Distributed Generation System:Adaptive Voltage Control Design and Stability Analysis.” In IEEE International Transactions on Energy Conversion ,Volume:29, Issue:1, pp.46-56, March 2014.
- [13] NagarajuPogaku, Milan Prodanovic, Timothy C.Green, “Modelling , Analysis and Testing of Autonomous Operation of an Inverter-Based Microgrid.” In IEEE International Transactions on Power Electronics, Volume:22, Issue:2, pp.613-625, March 2007.
- [14] XiaonanLu,KaiSun,Josep M Guerrero, Juan C.Vasquez, Lipei Huang and Jianhui Wang, “Stability Enhancement Based on Virtual Impedance for DC Microgrids With Constant Power Loads.” In IEEE International Transactions on Smart Grid, Volume:6, Issue:6, pp.2770-2783, November 2015.
- [15] TrudieWang ,Daniel O’Neill and HarehKamath, “Dynamic Control and Optimization of Distributed Energy Resources in a Microgrid.” In IEEE International Transactions on Smart Grid, Volume:6, Issue:6, pp.2784-2894, November 2015.
- [16] SarinaAdhikari,Fangxing Li and Huijuan Li, “P-Q and P-V Control of Photovoltaic Generators in Distribution Systems.” In IEEE International Transactions on Smart Grid, Volume:6, Issue:6, pp.2929-2941, November 2015.
- [17] XiongLiu,Peng Wang and Poh Chiang Loh, “Hybrid AC/DC Microgrid and Its Coordination Control.” In IEEE International Transactions on Smart Grid, Volume:2, Issue:2, pp.278-286, June 2011.
- [18] Abhinav Kumar Singh Ravindra Singh and BikashC.Pal. “Stability Analysis of Networked Control in Smart Grids.” In IEEE International Transactions on Smart Grid, Volume:6, Issue:1, pp.381-390, January 2015.
- [19] NavidEghtedarpour and EbrahimFarjah, “Power Control and Management in a Hybrid AC/DC Microgrid.” In IEEE International Transactions on Smart Grid, Volume:5, Issue:3, pp.1494-1505, May 2014.
- [20] S.Mishra, G.Malleshm and A.N.Jha, “Design of Controller and Communication for Frequency Regulation Of A Smart Microgrid.” In IET Transactions on Renewable Power Generation , Volume:6, Issue:4, pp.248-258, January 2012.
- [21] Khalil,H.K.:in ‘Nonlinear Systems’(Prentice-Hill.1996),2 ndEdn.
- [22] Carlos Meza Benavides, “Analysis and Control of a Single-Phase Single-Stage Grid-Connected Photovoltaic Inverter.”UniversitatPolitecnica de Catalunya,PhD Program.
- [23] Claudio A.Canizaresand Rodrigo Palma-Behnke, “Trends in MicrogridContro.” In IEEE International Transactions on Smart Grid, Volume:5, Issue:4, pp.1905-1919, July 2014.
- [24] Fangxing Li, Wei Qiao, Hongbin Sun, Hui Wan, JianhuiWang,YanXia,ZhaoXu and Pei Zhang , “Smart Transmission Grid Vision and Framework.” In IEEE International Transactions on Smart Grid, Volume:1, Issue:2, pp.168-177, September 2010.
- [25] Wenbo Shi, XiaorongXie, Chi-Cheng Chu and RajiGadh, “Distributed Optimal Energy Management in Microgrids.” In IEEE International Transactions on Smart Grid, Volume:6, Issue:3, pp.1137-1146, May 2015.
- [26] Dan Wu, Fen Tang,TomislavDragicovic,JosepM.Guerrero and Juan C.Vasquez, “Coordinated Control Based ON Bus-Signaling and Virtual Inertia for Islanded DC Microgrids.” In IEEE International Transactions on Smart Grid, Volume:6, Issue:6, pp.2627-2638, November 2015.



ISSN No: 2348-4845

# International Journal & Magazine of Engineering, Technology, Management and Research

*A Peer Reviewed Open Access International Journal*

- [27] KhosrowMoslehi and Ranjit Kumar, "A Reliability Perspective of the Smart Grid." In IEEE International Transactions on Smart Grid, Volume:1, Issue:1, pp.57-64, June 2010.